

## Supplementary Materials

Cation ordering, twinning and pseudo-symmetry: the study of a birefringent garnet  
with orthorhombic structure

Huifang Xu <sup>1\*</sup>, Shiyun Jin <sup>1,2</sup>, Seungyeol Lee <sup>1,3,4</sup> and Philip E. Brown <sup>1</sup>

<sup>1</sup>Department of Geoscience, University of Wisconsin-Madison, Madison, Wisconsin, 53706,  
USA

<sup>2</sup>Gemological Institute of America, 5355 Armada Drive, Carlsbad, CA 92008, USA

<sup>3</sup>USRA Lunar and Planetary Institute, 3600 Bay Area Boulevard, Houston, TX 77058, USA

<sup>4</sup>Department of Earth and Environmental Sciences, Chungbuk National University, Cheongju  
28644, Republic of Korea

\*Corresponding author: E-mail: [hfxu@geology.wisc.edu](mailto:hfxu@geology.wisc.edu)



Figure S1: The hand specimen collected from Stanley Butte, Graham County, Arizona showing euhedral crystals with brownish olive-green colour. Enlarged views of some crystals are illustrated in Figure S2.

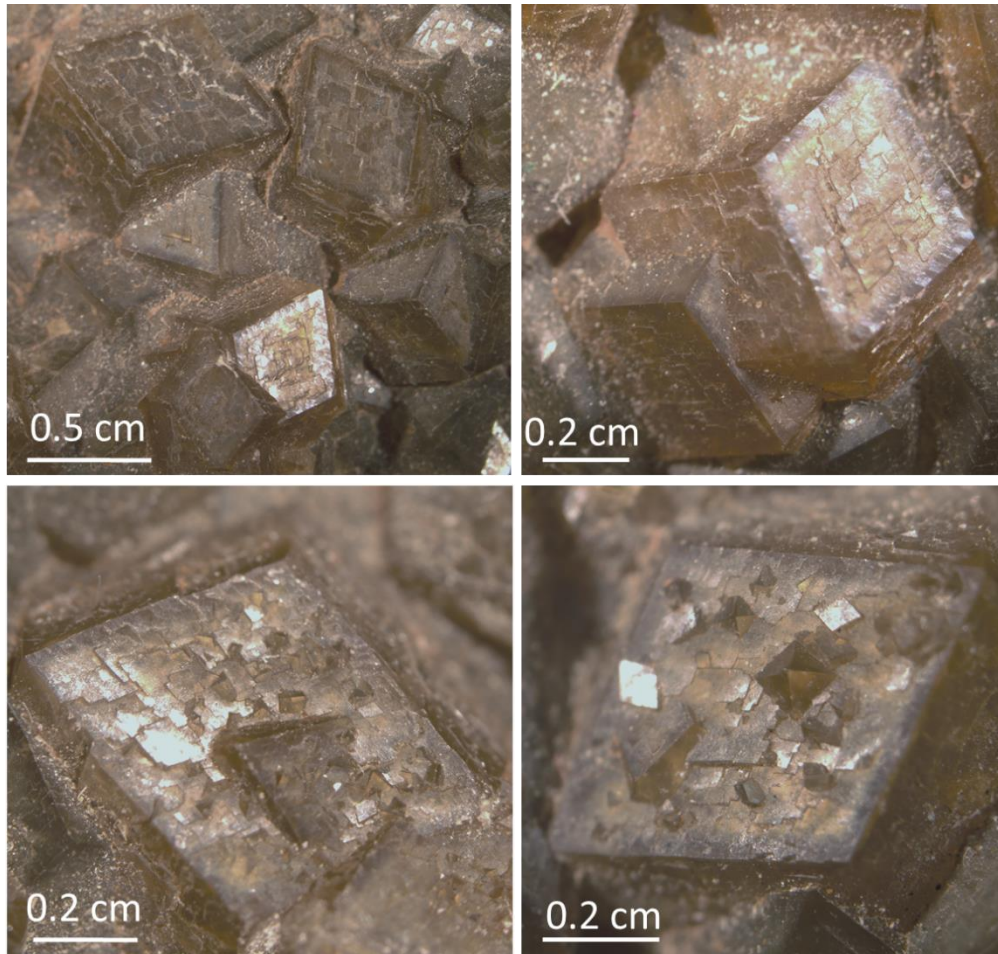


Fig. S2: Stereo-microscopic images showing the crystal  $\{110\}$  surfaces with vicinal planes and mosaic-like textures of the hand specimen.

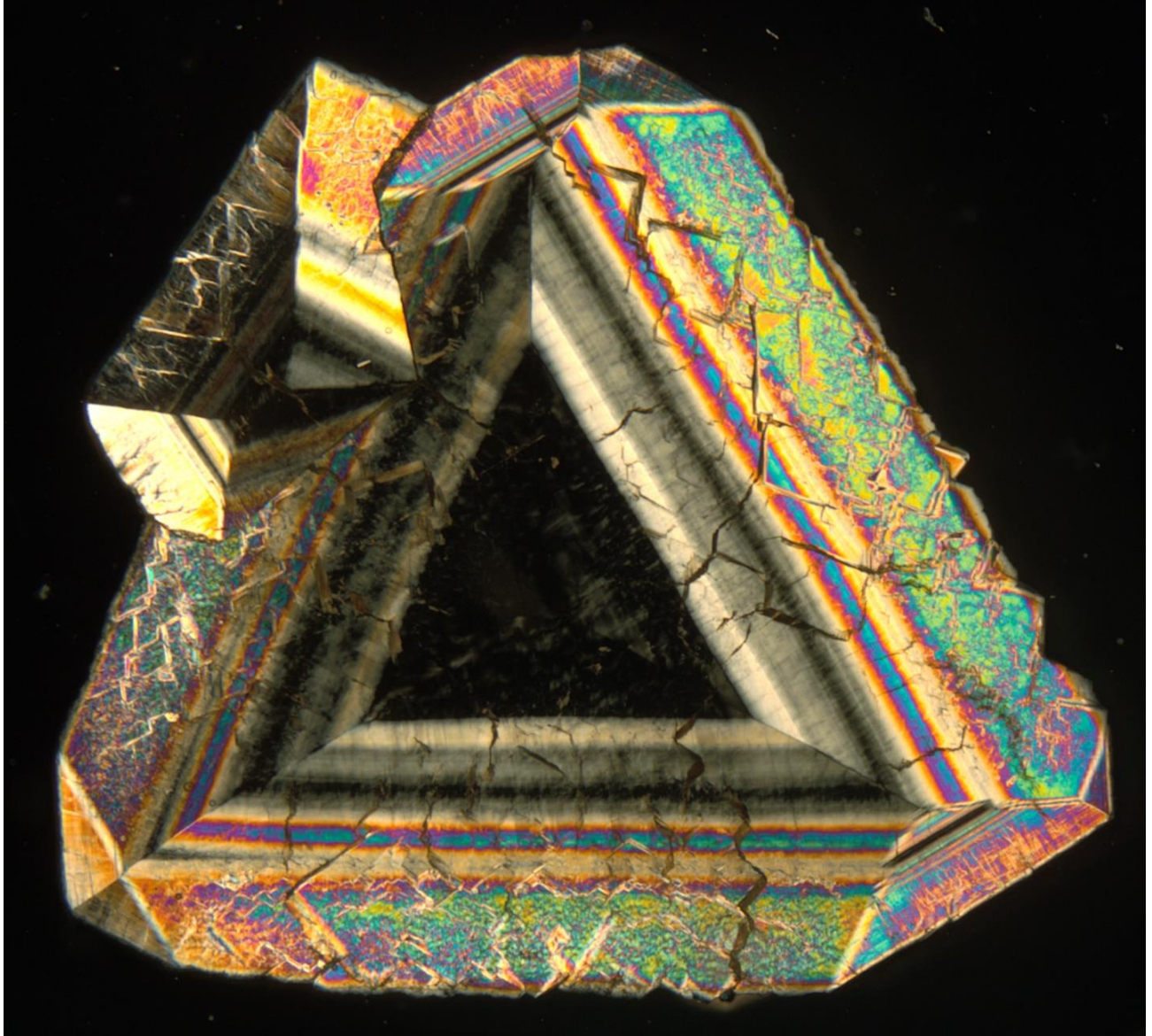


Fig. S3: Enlarged image of Figure 1A.



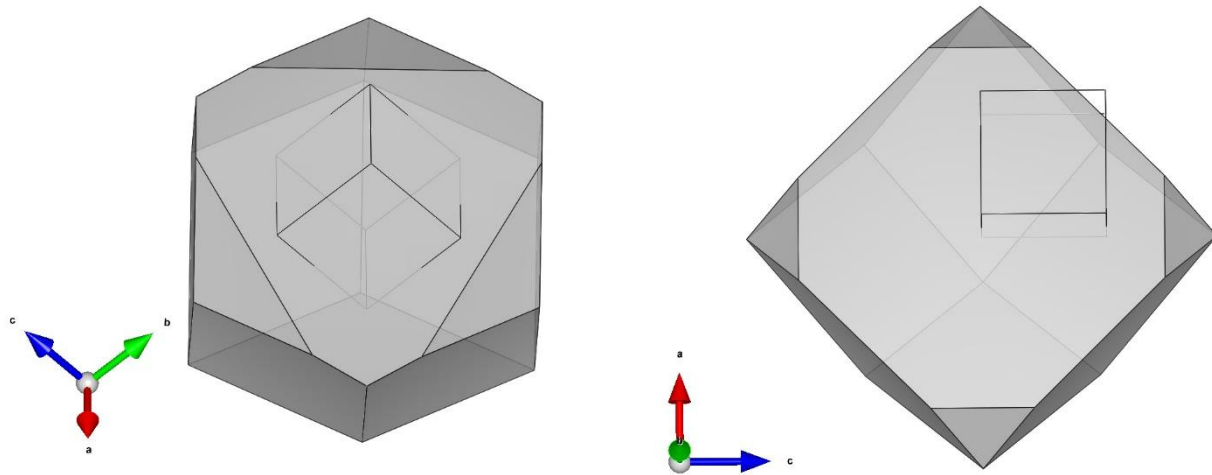


Fig. S4: Diagrams illustrate thin section cuttings for images 2A & S3 (left, ~ perpendicular to  $[111]$ ) and 2C (right, ~ perpendicular to  $b$ -axis). Cubic unit cells are also outlined.

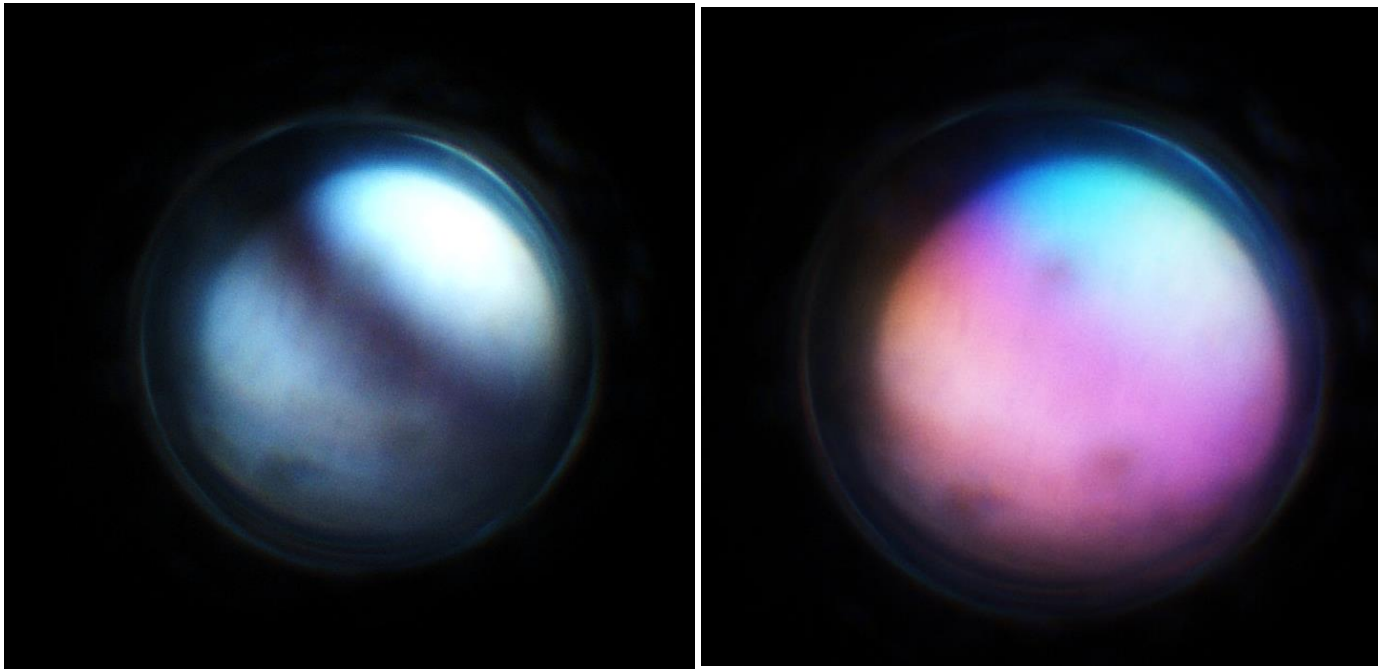


Fig. S5: Interference figure of the orthorhombic garnet slightly off one of the optical axes: left = without gypsum plate; right = with gypsum plate inserted.

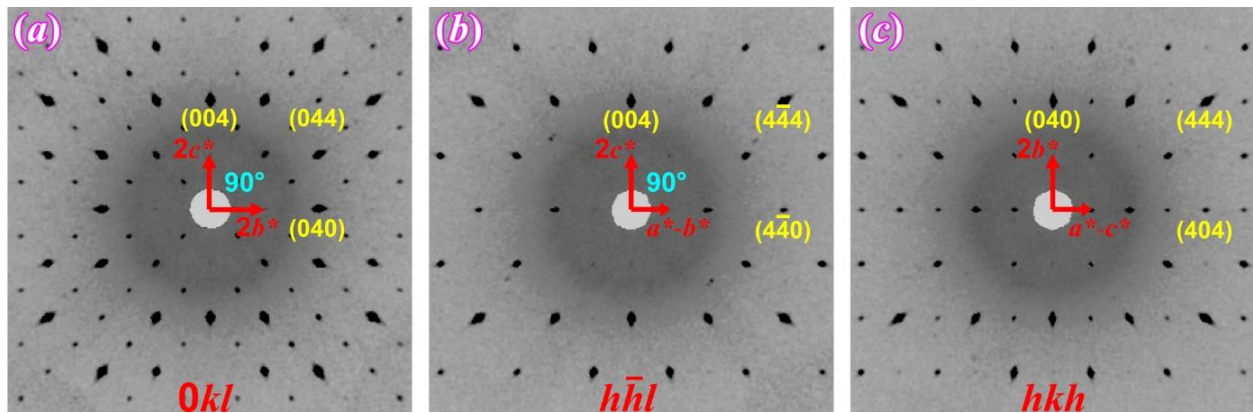


Figure S6: Reconstructed sections of X-ray diffraction data (simulated precession images) indicating the absence (presence) of glide planes in (100), (110) and  $(10\bar{1})$ .

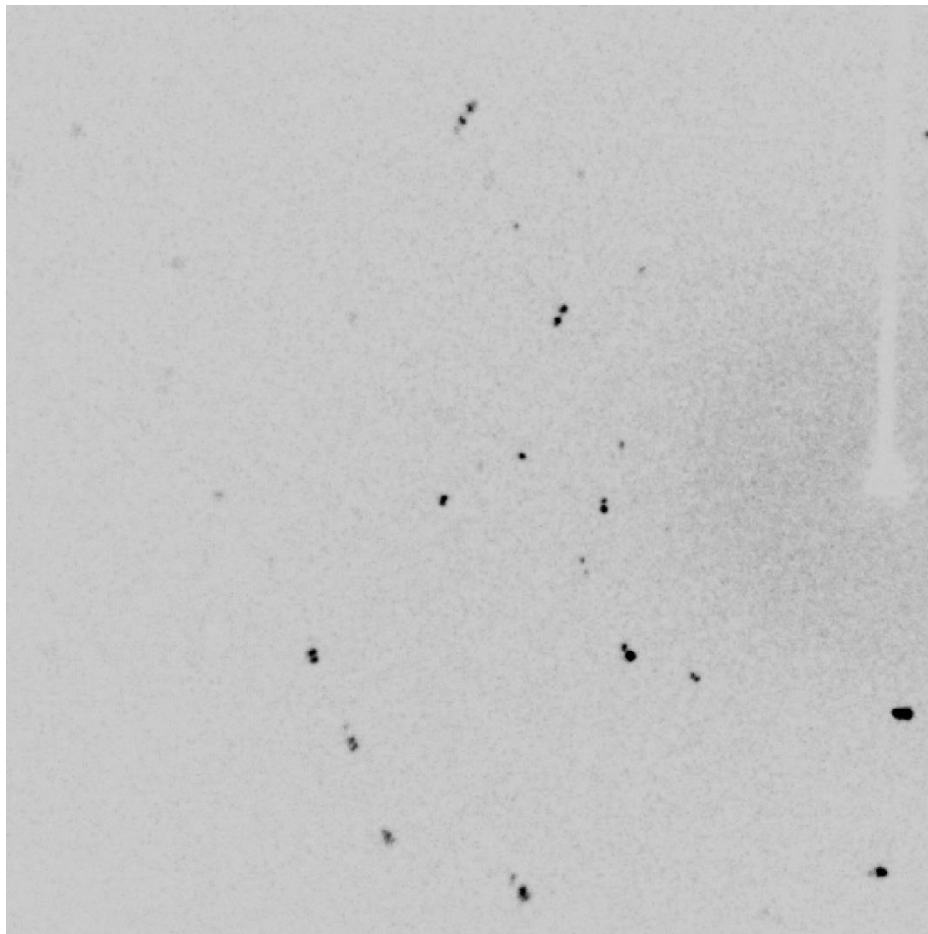


Figure S7: A diffraction frame from a screened crystal showing peak splitting due to pseudo-merohedral twinning, indicating the distortion from cubic symmetry of the orthorhombic garnet is large enough for any twinning to be easily detected in the single-crystal XRD.

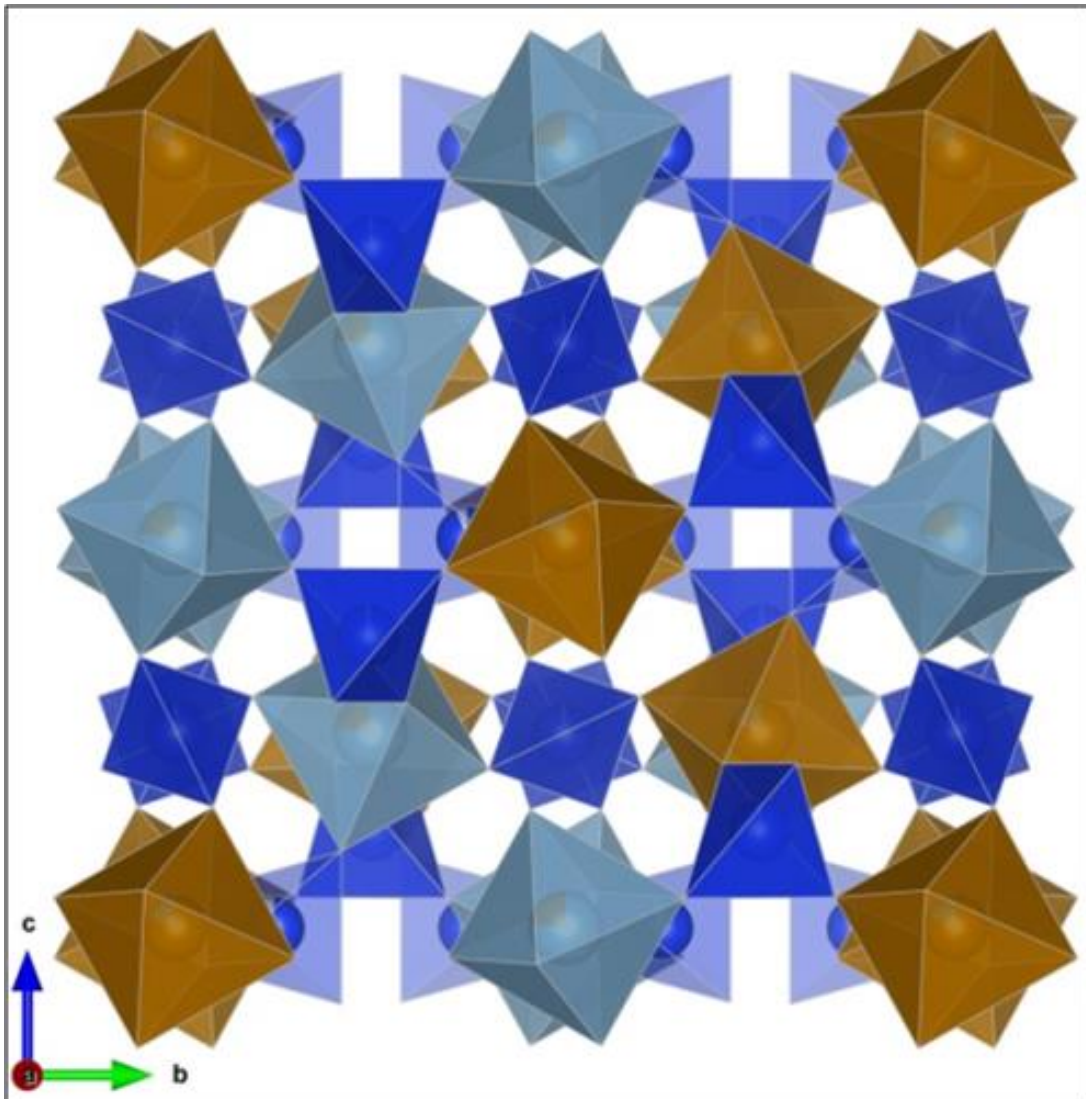


Figure S8: Orthorhombic garnet structure projected along  $a$ -axis. There are two octahedral sites, Y<sub>1</sub> (Fe, brown color) and Y<sub>2</sub> (Al, turquoise color). Atoms in the blue and light blue tetrahedra are Si<sub>1</sub> and Si<sub>2</sub> sites, respectively.

Table S1. Atom coordination and occupancies of the refined structure in the body-centered pseudo-cubic cell setting.

Site	Atom	Occ.	x	y	z	U <sub>equiv</sub>	Multiplicity
X <sub>1</sub>	Ca	1	0.24962(3)	0.37526(3)	0.50068(2)	0.00760(10)	16
X <sub>2</sub>	Ca	1	0	0.25	0.125	0.00787(13)	4
X <sub>3</sub>	Ca	1	0	0.25	0.625	0.00772(13)	4
Y <sub>1</sub>	Fe	0.804(3)	0	0	0	0.00590(12)	8
	Al	0.196(3)					
Y <sub>2</sub>	Al	0.779(3)	0	0	0.5	0.00458(17)	8
	Fe	0.221(3)					
Si <sub>1</sub>	Si	0.987(2)	0.24871(3)	0.12523(3)	0.50188(3)	0.00558(14)	16
Si <sub>2</sub>	Si	0.936(2)	0	0.25	0.37632(4)	0.00469(18)	8
O <sub>1</sub>	O	1	0.65182(8)	0.03911(8)	0.04540(8)	0.0095(3)	16
O <sub>2</sub>	O	1	0.04825(8)	0.65426(8)	0.03938(8)	0.0101(3)	16
O <sub>3</sub>	O	1	0.03821(8)	0.04671(7)	0.65148(8)	0.0091(3)	16
O <sub>4</sub>	O	1	0.34486(7)	0.53948(8)	0.45162(8)	0.0092(3)	16
O <sub>5</sub>	O	1	0.04656(8)	0.34807(8)	0.46275(8)	0.0098(3)	16
O <sub>6</sub>	O	1	0.46078(8)	0.04677(8)	0.34455(8)	0.0093(3)	16



Table S2. Anisotropic temperature parameters of atoms in the refined structure.

		U <sup>11</sup>	U <sup>22</sup>	U <sup>33</sup>	U <sup>12</sup>	U <sup>13</sup>	U <sup>23</sup>
X <sub>1</sub>	Ca	0.00786(17)	0.00584(17)	0.00911(19)	0.00117(14)	0.00097(9)	-0.00002(9)
X <sub>2</sub>	Ca	0.00832(18)	0.00832(18)	0.0070(3)	0.0020(2)	0	0
X <sub>3</sub>	Ca	0.00825(18)	0.00825(18)	0.0066(3)	0.0002(2)	0	0
Y <sub>1</sub>	Fe	0.0056(2)	0.0055(2)	0.0066(2)	0.00108(13)	0.00002(10)	-0.00009(10)
Y <sub>2</sub>	Al	0.0042(3)	0.0045(3)	0.0050(3)	0.0012(2)	-0.00002(15)	-0.00048(15)
Si <sub>1</sub>	Si	0.0052(2)	0.0050(2)	0.0066(3)	0.00114(19)	0.00012(13)	0.00015(13)
Si <sub>2</sub>	Si	0.0048(3)	0.0049(3)	0.0044(4)	0.0009(2)	0	0
O <sub>1</sub>	O	0.0091(5)	0.0094(5)	0.0101(5)	0.0017(4)	0.0004(4)	-0.0008(4)
O <sub>2</sub>	O	0.0095(5)	0.0088(5)	0.0119(5)	0.0010(4)	-0.0005(4)	0.0011(4)
O <sub>3</sub>	O	0.0081(4)	0.0095(5)	0.0096(5)	0.0007(4)	-0.0005(4)	0.0004(4)
O <sub>4</sub>	O	0.0090(5)	0.0087(5)	0.0099(5)	0.0012(4)	0.0000(4)	-0.0009(4)
O <sub>5</sub>	O	0.0086(5)	0.0096(5)	0.0113(5)	0.0017(4)	0.0006(4)	0.0009(4)
O <sub>6</sub>	O	0.0092(5)	0.0089(4)	0.0099(5)	0.0004(3)	0.0000(4)	-0.0003(4)

Table S3: Powder XRD data for the orthorhombic garnet ( $hkl^c$ : body-centered cell setting,  $hkl^o$ :  $Fddd$  cell setting)

$I_{obs}$	$d_{obs}$	$d_{calc}$	$I_{calc}$	$hkl^c$	$hkl^o$	$I_{obs}$	$d_{obs}$	$d_{calc}$	$I_{calc}$	$hkl^c$	$hkl^o$
1.4	8.452	8.4605	4.0	0 1 1	1 1 1			1.6632	12.1	4 0 -6	2 0 10
		4.8930	1.7	1 1 -2	1 1 3			1.6592	25.7	0 6 4	4 6 4
1.1	4.885	4.8767	1.4	1 1 2	3 1 1	<b>25.6</b>	<b>1.657</b>	1.6593	25.2	0 4 6	6 4 6
		4.2411	3.5	2 0 -2	0 0 4			1.6555	13.1	4 0 6	10 0 2
6.5	4.225	4.2303	11.2	0 2 2	2 2 2			1.6310	1.0	3 3 -6	3 3 9
		4.2199	3.0	2 0 2	4 0 0	1.1	1.629	1.6298	1.5	2 5 -5	3 5 7
		3.7835	1.1	0 3 1	1 3 1			1.6024	30.8	4 2 -6	2 2 10
0.8	3.780	3.7838	1.1	0 1 3	3 1 3			1.6006	29.7	2 4 -6	4 4 8
		3.2000	1.5	1 3 -2	1 3 3			1.6000	29.5	2 6 -4	2 6 6
1.2	3.192	3.1911	1.4	2 1 3	5 1 1	<b>67.3</b>	<b>1.597</b>	1.5977	30.4	2 6 4	6 6 2
		2.9911	52.6	0 4 0	0 4 0			1.5972	29.6	2 4 6	8 4 4
<b>56.3</b>	<b>2.988</b>	2.9914	100.0	0 0 4	4 0 4			1.5955	29.2	4 2 6	10 2 2
		2.8235	0.6	1 1 -4	3 1 5			1.4955	11.1	0 8 0	0 8 0
0.5	2.819	2.8202	0.3	0 3 3	3 3 3	<b>16.8</b>	<b>1.494</b>	1.4957	21.9	0 0 8	8 0 8
		2.8172	0.5	1 1 4	5 1 3			1.4736	0.9	1 4 -7	6 4 8
		2.6810	45.8	2 0 -4	2 0 6	1.2	1.471	1.4732	1.4	1 7 4	5 7 3
		2.6754	91.6	0 4 2	2 4 2			1.4720	0.7	1 4 7	8 4 6
<b>100</b>	<b>2.671</b>	2.6755	94.3	0 2 4	4 2 4			1.4086	0.5	5 3 -6	10 2 6
		2.6702	46.2	2 0 4	6 0 2	1.0	1.408	1.4066	1.0	2 2 -8	12 0 0
		2.5563	3.4	3 2 -3	0 2 6			1.3405	6.8	4 0 -8	4 0 12
		2.5545	11.1	2 3 -3	1 3 5			1.3377	13.2	0 8 4	4 8 4
7.1	2.549	2.5475	4.4	2 3 3	5 3 1	14.9	1.336	1.3377	13.6	0 4 8	8 4 8
		2.5458	3.6	3 2 3	6 2 0			1.3351	6.6	4 0 8	12 0 4
		2.4465	42.4	2 2 -4	2 2 6			1.3081	8.1	4 2 -8	4 2 12
		2.4444	20.5	-2 4 2	0 4 4			1.3068	7.5	2 4 -8	6 4 10
<b>45.1</b>	<b>2.439</b>	2.4403	20.0	2 4 2	4 4 0	<b>17.3</b>	<b>1.304</b>	1.3061	8.2	2 8 -4	2 8 6
		2.4384	41.2	2 2 4	6 2 2			1.3048	7.3	2 8 4	6 8 2

14.6	2.3453	2.3521	4.5	3 1 -4	1 1 7	9.2	1.274	1.3043	8.1	2 4 8	10 4 6
		2.3484	3.9	1 3 -4	3 3 5			1.3031	7.9	4 2 8	12 2 4
		2.3479	6.9	1 4 -3	2 4 4			1.2781	4.6	-6 4 6	0 4 12
		2.3451	6.8	1 4 3	4 4 2			1.2772	9.5	4 6 -6	2 6 10
		2.3448	10.4	1 3 4	5 3 3			1.2737	9.8	4 6 6	10 6 2
		2.3412	10.2	3 1 4	7 1 1			1.2729	4.9	6 4 6	12 4 0
14.2	2.184	2.1883	9.5	2 1 -5	3 1 7	14.4	1.110	1.1133	4.6	6 4 -8	2 4 14
		2.1864	6.8	1 2 -5	4 2 6			1.1129	2.8	4 0 -10	6 0 14
		2.1852	8.6	1 5 -2	1 5 3			1.1125	4.2	4 6 -8	4 6 12
		2.1837	4.5	1 5 2	3 5 1			1.1121	4.5	4 8 -6	2 8 10
		2.1828	6.5	1 2 5	6 2 4			1.1109	5.4	0 10 4	4 10 4
		1.9450	5.4	3 2 -5	2 2 8			1.1109	5.2	0 4 10	10 4 10
23.7	1.938	1.9436	7.2	2 3 -5	3 3 7	15.6	1.091	1.1098	4.2	4 8 6	10 8 2
		1.9425	2.7	2 5 -3	1 5 5			1.1094	4.6	4 6 8	12 6 4
		1.9426	8.3	1 1 -6	5 1 7			1.1091	2.4	4 0 10	14 0 6
		1.9412	5.6	-1 6 1	0 6 2			1.1087	4.1	6 4 8	14 4 2
		1.9406	5.5	1 6 1	2 6 0			1.0941	7.2	4 2 -10	6 2 14
		1.9394	7.9	2 5 3	5 5 1			1.0931	7.0	2 4 -10	8 4 12
8.2	1.889	1.9395	13.7	1 1 6	7 1 5	8.7	1.056	1.0926	6.9	2 10 -4	2 10 6
		1.9385	3.4	2 3 5	7 3 3			1.0919	7.1	2 10 4	6 10 2
		1.9372	5.1	3 2 5	8 2 2			1.0914	6.8	2 4 10	12 4 8
		1.8948	3.3	2 0 -6	4 0 8			1.0905	7.0	4 2 10	14 2 6
		1.8918	6.5	0 6 2	2 6 2			1.0603	4.9	8 0 -8	0 0 16
		1.8919	6.1	0 2 6	6 2 6			1.0576	19.9	0 8 8	8 8 8
8.0	1.726	1.8891	3.3	2 0 6	8 0 4			1.0550	5.0	8 0 8	16 0 0
		1.7299	13.7	4 4 -4	0 4 8						
		1.7242	12.9	4 4 4	8 4 0						

## Appendix

A series of diffraction data of twinned orthorhombic crystals of various proportions are simulated to study the effect of pseudo-merohedral twinning on the structure refinement. The single-crystal data of the orthorhombic structure is simulated using JANA2006 program with a noise level of 1. The data is then multiplied with a twin matrix and added to the original data at a certain ratio. Each resulting simulated data is represented by a 6-digit number which indicates the relative proportion of each individual twin domain ( $t_{oo}$ ,  $t_{od}$ ,  $t_{od'}$ ,  $t_{ao}$ ,  $t_{ad}$ ,  $t_{ad'}$ ). For example, 111111 is an intergrowth of TD<sub>oo</sub>, TD<sub>od</sub>, TD<sub>od'</sub>, TD<sub>ao</sub>, TD<sub>ad</sub>, TD<sub>ad'</sub> twin domains with same volume; 200100 is an intergrowth of TD<sub>oo</sub> and TD<sub>ao</sub> twin domains with 2:1 volume ratio, but without TD<sub>od</sub>, TD<sub>od'</sub>, TD<sub>ad</sub>, TD<sub>ad'</sub> domains. Although higher (pseudo-)symmetry may be present, we refined all the simulated diffraction data as a single crystal  $I\bar{1}$  structure. The resulting Fe occupancies of each Y site are listed in Table A1, along with the R factors of each structure refinement. If higher pseudo-symmetry is present, equivalent Y sites are coded with the same color.

The structure 100100 shows no Fe-Al ordering between Y<sub>1</sub> and Y<sub>2</sub> sites, but the symmetry is still orthorhombic. As discussed in the main text, the (100) glide plane twin law would only switch the positions of Y<sub>1</sub> and Y<sub>2</sub>, but keep the Si sites unchanged, which is why even though the Y<sub>1</sub> and Y<sub>2</sub> shows same occupancy, they are still symmetrically different sites. Structure 200100 obviously shows an orthorhombic structure with less ordered Y sites. Structure 111000 shows a [111] 3-fold rotoinversion symmetry. Structure 110110 shows pseudo-tetragonal  $I4_1/acd$  space group symmetry with all Y sites equivalent to each other. And with all six twin domains of equal volume to each other, the structure 111111 restores all the symmetry elements in the  $Ia\bar{3}d$  space group. It needs to be emphasized that all this pseudosymmetry produced by a certain twin domain component would fail any symmetry test regarding the extinction conditions. All the twinned crystals show no systematic extinctions required for screw axes and glide planes.

The paired-occupancy pattern as discussed in the main text are not exactly followed in the refined structure. This should be expected since the “average” structure of all the twin domains is not really an average of each site in the structure, and there is no symmetry constraint to make the occupancies equal to each other. The intensity of a certain reflection from a single crystal is



proportional to the square of the structure factor, whereas the reflection from a twinned crystal is the arithmetic mean of the intensities from different domains. The difference between Fe occupancies in  $Y_{1_1}$  and  $Y_{1_3}$  can be up to about 0.1 in structure 210000 and 510000 (refined from simulated twinned diffraction data) (Table A1). It is also interesting that the fake  $I\bar{1}$  structure can show an even wider range of Fe occupancies than the real orthorhombic structure, even though the average order between  $Y_1$  and  $Y_2$  is always lower in the  $I\bar{1}$  structures. The highest Fe ordering in the limited variations we tested is 0.888 of  $Y_{1_3}$  site in the structure 210000 (refined from simulated twinned diffraction data) (Table A1), and the lowest is 0.146 of  $Y_{2_4}$  in the same structure.

Table A1: Fe occupancies of the structures refined from simulated diffraction pattern of twinned crystals. The 6-digit number gives the relative proportion of each individual twin domain (TD<sub>00</sub>, TD<sub>01</sub>, TD<sub>02</sub>, TD<sub>03</sub>, TD<sub>04</sub>, TD<sub>05</sub>). The difference between the mean occupancies over each quartet of octahedra ( $X_{Oct1}-X_{Oct2}$  as defined by Shtukenberg et al, 2005) is also listed in the table for each structure.

Site	Coordinate	Twin Domains and Their Proportions					
		100000	100100	200100	110000	210000	510000
Y <sub>1_1</sub>	(0,0,0)	0.8118(8)	0.501(11)	0.666(10)	0.841(7)	0.799(6)	0.800(5)
Y <sub>1_2</sub>	(1/2,0,0)	0.8121(8)	0.497(11)	0.667(10)	0.551(7)	0.676(6)	0.753(5)
Y <sub>1_3</sub>	(1/4,1/4,1/4)	0.8137(8)	0.505(11)	0.673(10)	0.843(7)	0.888(6)	0.887(5)
Y <sub>1_4</sub>	(1/4,1/4,3/4)	0.8140(8)	0.505(11)	0.675(10)	0.484(7)	0.607(6)	0.690(5)
Y <sub>2_1</sub>	(0,1/2,0)	0.2288(8)	0.497(11)	0.347(10)	0.190(6)	0.236(6)	0.240(5)
Y <sub>2_2</sub>	(1/2,1/2,0)	0.2284(8)	0.500(11)	0.347(10)	0.482(7)	0.362(6)	0.288(4)
Y <sub>2_3</sub>	(1/4,3/4,1/4)	0.2297(8)	0.504(11)	0.348(10)	0.549(7)	0.427(6)	0.349(5)
Y <sub>2_4</sub>	(3/4,1/4,1/4)	0.2287(8)	0.505(11)	0.349(10)	0.188(6)	0.146(6)	0.151(4)
R factor %		0.38	5.48	4.58	2.95	2.63	1.92
Symmetry		Orthorhombic	Orthorhombic	Orthorhombic	Monoclinic	Triclinic	Triclinic
$X_{Oct1}-X_{Oct2}$		0.584	0.0005	0.3225	0.3275	0.44975	0.5255
Site	Coordinate	Twin Domains and Their Proportions					
		111000	302010	302100	321000	110110	111111
Y <sub>1_1</sub>	(0,0,0)	0.823(9)	0.815(8)	0.767(9)	0.811(8)	0.490(13)	0.498(13)
Y <sub>1_2</sub>	(1/2,0,0)	0.409(9)	0.576(8)	0.488(9)	0.604(8)	0.487(13)	0.489(13)
Y <sub>1_3</sub>	(1/4,1/4,1/4)	0.857(9)	0.750(8)	0.802(9)	0.879(8)	0.501(13)	0.504(13)
Y <sub>1_4</sub>	(1/4,1/4,3/4)	0.395(9)	0.663(8)	0.553(9)	0.519(8)	0.515(13)	0.513(13)
Y <sub>2_1</sub>	(0,1/2,0)	0.407(9)	0.511(8)	0.530(9)	0.283(8)	0.501(13)	0.499(13)
Y <sub>2_2</sub>	(1/2,1/2,0)	0.408(9)	0.158(8)	0.250(9)	0.367(8)	0.498(13)	0.495(13)
Y <sub>2_3</sub>	(1/4,3/4,1/4)	0.396(9)	0.211(8)	0.231(9)	0.452(8)	0.514(13)	0.510(13)
Y <sub>2_4</sub>	(3/4,1/4,1/4)	0.394(9)	0.435(8)	0.477(9)	0.210(8)	0.498(13)	0.495(13)
R factor %		3.87	3.54	4.28	3.54	5.90	6.11
Symmetry		p-Trigonal	Triclinic	Triclinic	Triclinic	p-Tetragonal	p-Cubic
$X_{Oct1}-X_{Oct2}$		0.21975	0.37225	0.2805	0.37525	-0.0045	0.00125